# Edge Detection from Spectral Phase Data

by Alexander Reynolds

A thesis submitted in partial fulfillment
of the requirements for the degree of
Honors Bachelor of Science in Mathematics

Arizona State University

April 8, 2016

*© 2016, Alexander Reynolds*
http://reynoldsalexander.com

*To Ernie Reynolds*

# Acknowledgments

This thesis would not have been possible without the help of a few individuals whom I am obliged to recognize for their help and friendship. First and foremost, I would have never expected to be where I am today without the constancy from my partner, Kim Jones. Your encouragement was invaluable for my embarking on a degree in mathematics, and your continuous support has allowed me to take risks throughout my undergraduate career that I would have never been able to alone. I owe similar praise to my family, and especially my mother for the countless second chances she has given me.

I am grateful to my adviser Dr. Anne Gelb, whose patience I have tried over these many months. Our rambling discussions have given me a greater understanding of the interconnections of academia and industry and have inspired me to reach farther with my career goals. Many thanks are also due to Dr. Cochran for his innate ability to break apart a problem and give helpful suggestions at every turn, and to Dr. Viswanathan for his quick responses to my many questions, especially at the start of my research.

This work was started over the summer of 2015 as part of Arizona State University's Mentoring through Critical Transition Points (MCTP) program. I would like to thank Dr. Eric Kostelich for his dedication in running this program at ASU and the National Science Foundation for their support of the MCTP program. Finally, I would have not been able to make any strides on such a project without the help of my colleagues, Shane and Rachel, who have helped me comb through code on numerous occasions until our eyes bled. Thank you.

# Abstract

The detection and characterization of transients in signals is important in many wide-ranging applications from computer vision to audio processing. Edge detection on images is typically realized using small, local, discrete convolution kernels, but this is not possible when samples are measured directly in the frequency domain. The concentration factor edge detection method was therefore developed to realize an edge detector directly from spectral data.

This thesis explores the possibilities of detecting edges from the phase of the spectral data, that is, without the magnitude of the sampled spectral data. Prior work has demonstrated that the spectral phase contains particularly important information about underlying features in a signal. Furthermore, the concentration factor method yields some insight into the detection of edges in spectral phase data. An iterative design approach was taken to realize an edge detector using only the spectral phase data, also allowing for the design of an edge detector when phase data are intermittent or corrupted. Problem formulations showing the power of the design approach are given throughout. A post-processing scheme relying on the difference of multiple edge approximations yields a strong edge detector which is shown to be resilient under noisy, intermittent phase data. Lastly, a thresholding technique is applied to give an explicit enhanced edge detector ready to be used. Examples throughout are demonstrate both on signals and images.

# Contents

# List of Figures

# List of Tables

# Chapter 1

# Edge Detection

## 1.1 Introduction

The detection and characterization of transients in signals is important in many wide-ranging applications from computer vision to audio processing. In machine learning, edge detection can be utilized to reduce the size of data sets by keeping only structurally specific information for pattern recognition or object classification. In computer vision applications, finding and characterizing the types of edges allows us to infer information for scene recognition and object tracking. Edges are also used as reference points for stereo matching in machine vision, where multiple image sensors are used together to provide accurate depth and distance references. More basic sensors which measure some signal over time, like microphones, laser vibrometers, infrared sensors, and the like, can utilize transients as triggers for sending out warning signals in electrical and mechanical systems. Mathematically, finding jump locations in discontinuous functions is essential for strong accuracy in numerical and spectral methods for PDE.

Most of the examples listed collect information in the physical domain. However, in some applications such as medical imaging, telemetry, and radar, data are collected directly in the spectral domain. Spectral data give global information over the scene, typically holding redundant information. However, the global behavior of spectral data constitutes a problem for edge detection, since edges are very localized phenomena.

This thesis begins with a discussion of spectral data and its use in edge detection, outlining the concentration factor method developed in [1]. The method is then expanded upon in [7] by introducing an iterative framework to compute problem-specific reconstruction schemes. Interference, cross-talk, distortions, and other errors can affect measurements so that a portion of the data is unusable. The iterative framework allows adaptation to these problems, and is here utilized to build edge reconstructions

when spectral data are interrupted in some band of frequencies and from phase data where the spectral magnitude is corrupted and expendable. Post-processing from [2] is then applied to these reconstructions to achieve operational detectors. Many sample problem formulations are given throughout with one-dimensional signals, and a few edge detectors built from these formulations are applied to two-dimensional images.

## 1.2 Spectral Data

In signal processing, spectral data are any set of data which describe the amplitude of various frequencies. Audio signals are a great example of functions which are readily described both in terms of the time domain and frequency domain: rhythm lives in the time domain, while tone lives in the frequency domain. We interact with sound in the frequency domain when we adjust bass frequencies on an equalizer. The mathematics of harmonic analysis allow us to translate back and forth between these two domains efficiently and effectively through the Fourier transform.

The Fourier series of a $2\pi$-periodic piecewise-smooth function $f\colon [-\pi,\pi) \to \mathbb{R}$ is given by the infinite sum

$$Sf(x) = \sum_{k=-\infty}^{\infty} \hat{f}_k e^{ikx}, \tag{1.1}$$

where the coefficients $\hat{f}_k$ are called the *Fourier coefficients* of $f$, defined by

$$\hat{f}_k = \frac{1}{2\pi}\int_{-\pi}^{\pi} f(x)e^{-ikx}\,dx. \tag{1.2}$$

As an abstract construction, Fourier series allow for a simple way to represent functions. However, an infinite series is, of course, unusable for computations; a partial sum is used instead. The *partial Fourier series* truncated at a natural number $N$ is

$$S_N f(x) = \sum_{|k|\le N} \hat{f}_k e^{ikx}. \tag{1.3}$$

Notice that the Fourier coefficients are complex numbers. Written in exponential form, $\hat{f}_k = A_k e^{i\varphi_k}$, where $A_k = |\hat{f}_k|$ is the *amplitude* and $\varphi_k = \arg(\hat{f}_k)$ is the *phase* of the $k$-th Fourier coefficient of $f$. In this thesis, the terms *Fourier coefficients*, *Fourier data*, and *spectral data* will be used interchangeably.

## 1.3 Edge Detection

For the purposes of this thesis, a signal is simply a one-dimensional piecewise smooth function, defined at every point in the domain. Edge detection is the detection of in-

stantaneous changes, or transients, in such a signal. Namely, we wish to find the discontinuities (also called *jumps* or *edges*) in the function and how large the jumps are.

**Definition 1** (Jump Function)**.** The *jump function* of a piecewise-smooth real-valued function $f$, denoted $[f](x)$, is the difference between the right and left hand limits of the function at every point $x$,

$$[f](x) = f(x^+) - f(x^-). \tag{1.4}$$

The jump function is non-zero only at a jump of the function, where it assumes the value of the jump. With finite discontinuities $\{\xi_j : j = 1,\dots,n\}$ where $[f](\xi_j)$ is the jump value at $\xi_j$, then the jump function can also be defined by

$$[f](x) = \sum_{j=1}^{n} [f](\xi_j)\delta_{\xi_j}(x), \tag{1.5}$$

where $\delta_\xi(x)$ is the Kronecker delta function, or indicator function, at $\xi$,

$$\delta_\xi(x) = \begin{cases} 1 & x = \xi, \\ 0 & x \neq \xi. \end{cases} \tag{1.6}$$

Dirichlet's convergence theorem relates the limits from (1.4) with the partial sum approximation of a piecewise-smooth function by

$$S_N f(x) \longrightarrow \frac{1}{2}\left(f(x^+) + f(x^-)\right) \text{ as } N \longrightarrow \infty. \tag{1.7}$$

In fact, the partial sum in (1.7) can be modified to instead converge to $[f](x)$ due to this relationship. This is the approach taken in [1] to find discontinuities in a function. The partial Fourier sum is modified by a function called a *concentration factor*, yielding the approximation to the jump function $[f]$ given by

$$S_N^\sigma[f](x) = \sum_{0<|k|\leq N} i\,\mathrm{sgn}(k)\sigma(k)\hat{f}_k e^{ikx} \approx [f](x). \tag{1.8}$$

In particular, we are interested admissible concentration factors [1] $\sigma$ which satisfy the *concentration property*:

$$S_N^\sigma[f](x) = [f](x) + \begin{cases} O\left(\frac{\log N}{N}\right) & d(x,\xi) \lesssim \frac{\log N}{N}, \\ O\left(\frac{\log N}{(Nd(x,\xi))^s}\right) & d(x,\xi) \gg \frac{1}{N}, \end{cases} \tag{1.9}$$

where $d(x,\xi)$ is the distance between $x$ and the nearest jump discontinuity $\xi$ and $s$ depends on the chosen concentration factor.The concentration property not only guarantees convergence to the jump function, but fast convergence as well.

Since we are interested in approximations, there are multiple families of solutions $\sigma$ with different convergence properties. Some examples of these admissible concentration factors are given in Table 1.1.

Table 1.1: Common analytic concentration factors as functions of $\eta = k/N$.

| **Factor** | **Expression** | **Remarks** |
|---|---|---|
| Trigonometric | $\sigma^T(\eta) = \frac{\pi \sin(\pi\eta)}{\mathrm{Si}(\pi)}$ | $\mathrm{Si}(\pi) = \int_0^\pi \frac{\sin(x)}{x}\,dx$ |
| Polynomial | $\sigma^P_\alpha(\eta) = p\pi\eta^p$ | $p$ is the order of the factor |
| Exponential | $\sigma^E_\alpha(\eta) = C\eta e^{\frac{1}{\alpha\eta(\eta-1)}}$ | $\alpha$ is the order |
| | | $C$ is a normalizing constant |
| | | $\frac{\pi}{C} = \int_{\frac{1}{N}}^{1-\frac{1}{N}} \exp(\frac{1}{\alpha\tau(\tau-1)})\,d\tau$ |

One representative of each concentration factor from Table 1.1, specifically $\sigma^P_{p=1}$, $\sigma^T$, and $\sigma^E_{\alpha=6}$, are plotted in Figure 1.1 along with the accompanying jump approximations $S^\sigma_N[r](x)$ of the ramp function $r$, defined in (2.1), exemplifying their respective properties: the low order polynomial factor shows some oscillations throughout the recovered domain, the trigonometric factor show decreased resolution around the jump, and the exponential factor has large oscillations but only local to the discontinuities.

Figure 1.1: Analytic factors with their corresponding jump responses $S^\sigma_N[r](x)$, $N = 64$.

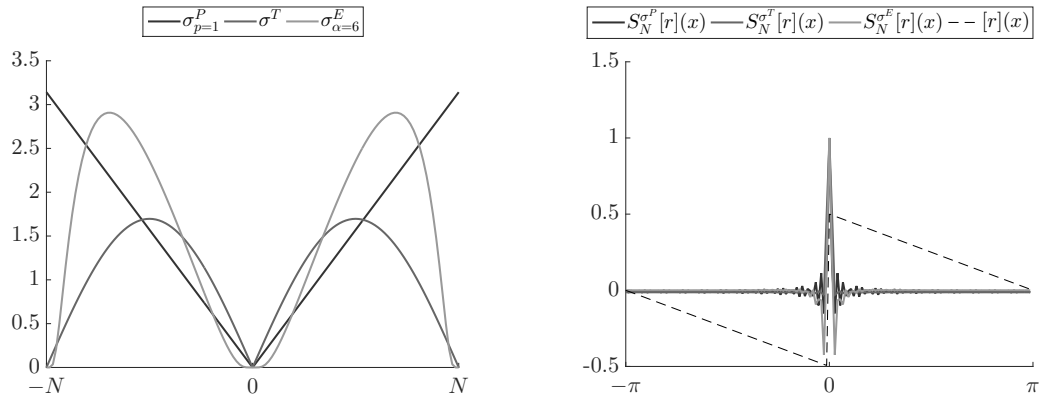

# Chapter 2

# Concentration Factor Design

The partial sum in (1.8) yields an approximation to $[f](x)$, and prior literature has focused on improving its accuracy. However, a new approach was taken in [7], developing an iterative method to build concentration factors with desired properties for a particular application, giving a highly customizable framework to build from. In [7] some analytic concentration factors were shown to be the solutions of this method under certain constraints.

## 2.1 Design Methods

For the development of the method, we assume a single discontinuity at $x = \xi \in (-\pi, \pi)$. The method can be easily generalized to include multiple jumps, as long as the jumps are sufficiently resolved, however, the error of the approximation increases with each additional jump. The approach starts by noting that the Fourier coefficients of a periodic piecewise-smooth function on $[-\pi, \pi)$ are related to those of a simple ramp function. The unit ramp function $r(x)$ with associated jump function $[r](x)$ on the interval $[-\pi, \pi)$ is given by

$$r(x) = \begin{cases} \frac{1}{2\pi}(-x-\pi) & x < 0, \\ \frac{1}{2\pi}(-x+\pi) & x \geq 0; \end{cases} \quad [r](x) = \delta_0(x) = \begin{cases} 1 & x = 0, \\ 0 & x \neq 0. \end{cases} \tag{2.1}$$

The Fourier coefficients of the ramp centered at $x = 0$ are

$$\hat{r}_k = \frac{1}{2\pi} \int_{-\pi}^{\pi} r(x) e^{-ikx} \, dx = \begin{cases} \frac{1}{2\pi i k} & k \neq 0, \\ 0 & k = 0. \end{cases} \tag{2.2}$$

**Definition 2** (Concentration Kernel Response)**.** The jump response associated with a concentration factor $\sigma$, denoted $W_0^\sigma(x)$, is defined as the partial sum jump approximation (1.8) of the unit ramp (2.2), viz.,

$$W_0^\sigma(x) \coloneqq S_N^\sigma[r](x) = \frac{1}{2\pi} \sum_{0<|k|\le N} \frac{\sigma(k)\,\mathrm{sgn}(k)}{k} e^{ikx}. \tag{2.3}$$

Higher order concentration kernels are similarly defined by the jump response at the $q$-th derivative of Bernoulli period functions, denoted $W_q^\sigma(x)$, viz.,

$$W_q^\sigma(x) \coloneqq \frac{1}{2\pi} \sum_{0<|k|\le N} \frac{\sigma(k)\,\mathrm{sgn}(k)}{i^q k^{q+1}} e^{ikx}. \tag{2.4}$$

The full derivations and motivation for these definitions can be found in [7]. These definitions are used to express (1.8) as a sum of these scaled and shifted kernels exactly. Integrating by parts on the Fourier coefficients of a piecewise-smooth function $f$ with a single jump discontinuity at $x = \xi \in (-\pi, \pi)$, we see

$$\begin{aligned}
\hat{f}_k &= \frac{1}{2\pi}\int_{-\pi}^{\pi} f(x)e^{-ikx}\,dx \\
&= \frac{1}{2\pi}\left(\int_{-\pi}^{\xi} f(x)e^{-ikx}\,dx + \int_{\xi}^{\pi} f(x)e^{-ikx}\,dx\right) \\
&= \frac{1}{2\pi ik}[f](\xi)e^{-ik\xi} + \frac{1}{ik}\int_{-\pi}^{\pi} f'(x)e^{-ikx}\,dx \\
&= \frac{1}{2\pi ik}[f](\xi)e^{-ik\xi} + O\left(\frac{1}{k^2}\right) \\
&= \hat{r}_k[f](\xi)e^{-ik\xi} + O\left(\frac{1}{k^2}\right),
\end{aligned} \tag{2.5}$$

where $[f](\xi)$ is the jump value at $x = \xi$.

So, the Fourier coefficients of $f$ look like scaled (by the jump height) and shifted (by the location of the jump) coefficients of the ramp $r$. We can be more precise by repeated integration by parts; specifically,

$$\hat{f}_k = \frac{1}{2\pi}\left(\frac{[f](\xi)}{ik} + \frac{[f'](\xi)}{(ik)^2} + \frac{[f''](\xi)}{(ik)^3} + \cdots\right)e^{-ikx}, \qquad k \neq 0. \tag{2.6}$$

Substituting this into the concentration partial sum (1.8), we deduce

$$S_N^\sigma[f](x) = [f](\xi)W_0^\sigma(x-\xi) + [f'](\xi)W_1^\sigma(x-\xi) + [f''](\xi)W_2^\sigma(x-\xi) + \cdots. \tag{2.7}$$

The concentration factors should emphasize the jump response $W_0^\sigma(x-\xi)$ while suppressing the higher order concentration kernels. Since we are interested in a function which yields the jump function, we want $W_0^\sigma(x-\xi) \approx \delta_\xi(x)$ to be similar to the Kronecker delta (1.6). Note that it suffices to require $W_0^\sigma(x) \approx \delta_0(x)$ since a shift in the jump location from $\xi$ to zero can be achieved by simply shifting the phase of the Fourier coefficients.

We therefore have a list of criteria that a concentration factor should adhere to. The design approach in [7] then consists of solving an iterative semidefinite program for a concentration factor $\sigma$ so that these conditions are upheld. A typical problem formulation takes the form

$$\begin{aligned} \min_{\sigma} \quad & \phi_0(\sigma) \\ \text{subject to} \quad & \phi_m(\sigma) = c_m \quad m = 1,\dots,M \\ & \psi_n(\sigma) \le d_n, \quad n = 1,\dots,N. \end{aligned} \tag{2.8}$$

The objective function $\phi_0$ is usually the $\ell_1$ or $\ell_2$ norm of $W_0^\sigma(x)$, so that we have a concentration factor which gives us a jump response with minimum spurious jumps:

$$\min_{\sigma} \quad \left\| W_0^\sigma(x) \right\|_i, \quad i = 1 \text{ or } 2.$$

Often the imposed constraints will include forcing the jump response to be 1 at the jump location, that is,

$$W_0^\sigma(x)\big|_{x=0} = 1.$$

Additional constraints may be to suppress the higher order kernels by enforcing

$$\left\| W_i^\sigma(x) \right\|_\infty \le \epsilon$$

for some tolerance $\epsilon > 0$, or imposing that the jump response should be small away from jumps by

$$\left| W_0^\sigma(x) \right|_{|x|\ge\delta} \le \epsilon$$

for some small $\delta$ neighborhood around 0. In [7], the formulation which minimizes the $\ell_2$ norm of $W_0^\sigma(x)$ and forces the jump response to be 1 at the jump location is shown to yield the concentration factor $\sigma_{p=1}^P$ from Table 1.1.

For an example of the process, we will consider problem formulations within this framework, and utilize the Matlab package `CVX` to solve the optimization problems. In these examples, and the rest of the paper, we will demonstrate the concentration factor

applied in a jump approximation to the function

$$f(x) = \begin{cases} \frac{3}{2} & -\frac{3\pi}{4} \le x < -\frac{\pi}{2}, \\ \frac{3}{5} - \frac{x}{2} + \sin(5x - \frac{1}{4}) & -\frac{\pi}{4} \le x < \frac{\pi}{8}, \\ \frac{11}{4}x - 5 & \frac{3\pi}{8} \le x < \frac{2\pi}{4}, \\ 0 & \text{otherwise.} \end{cases} \tag{2.9}$$

**Problem Formulation 1**

$$\begin{aligned} \min_{\sigma} \quad & \left\| W_0^{\sigma}(x) \right\|_2 \\ \text{subject to} \quad & W_0^{\sigma}(x)\big|_{x=0} = 1, \\ & \left| W_0^{\sigma}(x) \right|_{|x| \ge 0.2} \le 10^{-4}. \end{aligned} \tag{2.10}$$

This formulation yields the concentration factor, jump response, and jump approximation given in Figure 2.1. The jump response shows a quick decay away from jumps with the correct, normalized jump height due to the constraints in (2.10).

Figure 2.1: Formulation 1 solution $\sigma$, $W_0^{\sigma}(x)$, and $S_N^{\sigma}[f](x)$, with $N = 64$.

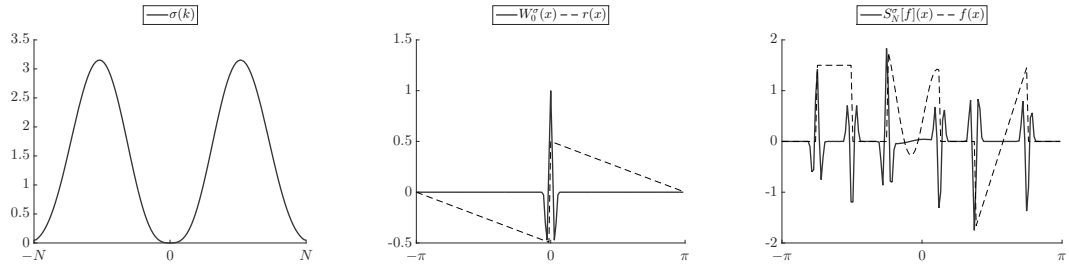


We can take a slightly different approach in our objective function. We can instead minimize

$$\left\| W_0^{\sigma}(x) - [r](x) \right\|,$$

where $[r](x)$ is given in (2.1). However, as $[r](x) = \delta_0(x)$, we may be asking for more precision around the jump location than our data allows. We can overcome this by substituting a regularized version of $[r](x)$, denoted $[r]_{\epsilon}(x)$, which depends on the number $2N+1$ of Fourier coefficients

$$[r]_{\epsilon}(x) := e^{-\left(\frac{N}{\sqrt{2}\pi}x\right)^2}. \tag{2.11}$$

The 2-norm is particularly useful in this situation, since we want the objective function to be as small as possible everywhere and the function $[r]_{\epsilon}(x)$ is smooth. Since the

jump response is sparse, we can additionally minimize $\lambda \left\| W_0^\sigma(x) \right\|_1$ with the objective function

$$\left\| W_0^\sigma(x) - [r](x) \right\|_2 + \lambda \left\| W_0^\sigma(x) \right\|_1$$

with $\lambda > 0$ free to choose depending on which norm should be emphasized more, that is, whether we want smoother conformity to $[r]_\epsilon(x)$ or a more sparse response.

**Problem Formulation 2**

$$\begin{aligned} \min_{\sigma} \quad & \left\| W_0^\sigma(x) - [r]_\epsilon(x) \right\|_2 + \lambda \left\| W_0^\sigma(x) \right\|_1 \\ \text{subject to} \quad & W_0^\sigma(x)\big|_{x=0} = 1. \end{aligned} \tag{2.12}$$

This problem formulation with $\lambda = 0.5$ yields the concentration factor, jump response, and jump approximation given in Figure 2.2. Minimizing this objective function keeps the jump response sparse while emphasizing closeness to $[r]_\epsilon(x)$.

Figure 2.2: Formulation 2 solution $\sigma$, $W_0^\sigma(x)$, and $S_N^\sigma[f](x)$, with $\lambda = 0.5$, $N = 64$.

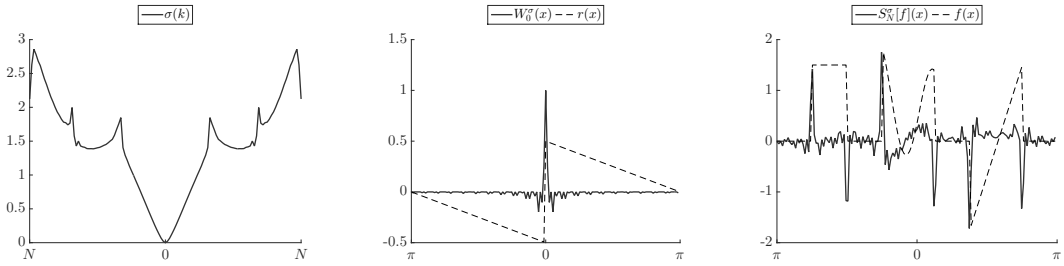


## 2.2 Intermittent Data

In application, spectral data can be corrupted in certain frequency bands, or can be simply intermittent throughout the frequency domain. One of the major benefits of the design approach is to create concentration factors with these missing bands or frequencies in mind. A simple constraint is added to the program to enforce that the concentration factor weights other frequencies instead of the missing ones. Specifically, the objective function is subjected to the constraint

$$\sigma[K] = 0$$

where $K$ is the set of missing frequencies so that $\hat{f}_k = 0$ when $k \in K$.

Note that this holds whether $K$ is a set of discrete points, or an interval, or multiple intervals in the sampled spectral space. Due to the missing frequencies, the resolution

of the recovered jump is typically reduced. However, spurious jumps away from the jump locations are considerably reduced by including the missing bands in the design process, as opposed to the analytic concentration factors which assume data throughout the full spectral space.

As an example of this design, consider the following problem formulation where the frequencies $K = \{k : 20 \le |k| \le 25\}$ are missing. In this case, about 10% of the frequencies are missing.

**Problem Formulation 3**

$$\begin{aligned} \min_{\sigma} \quad & \left\| W_0^{\sigma}(x) \right\|_2 \\ \text{subject to} \quad & W_0^{\sigma}(x)\big|_{x=0} = 1, \\ & \left| W_0^{\sigma}(x) \right|_{0.1 \le |x| \le 0.5} \le 10^{-1}, \\ & \sigma[K] = 0. \end{aligned} \tag{2.13}$$

In this formulation, the jump response is expected to be relatively narrow by enforcing that the oscillations around the jump are small. The concentration factor, jump response, and jump approximation from (2.13) are plotted in Figure 2.3.

Figure 2.3: Formulation 3 solution $\sigma$, $W_0^{\sigma}(x)$, and $S_N^{\sigma}[f](x)$, with $N = 64$.

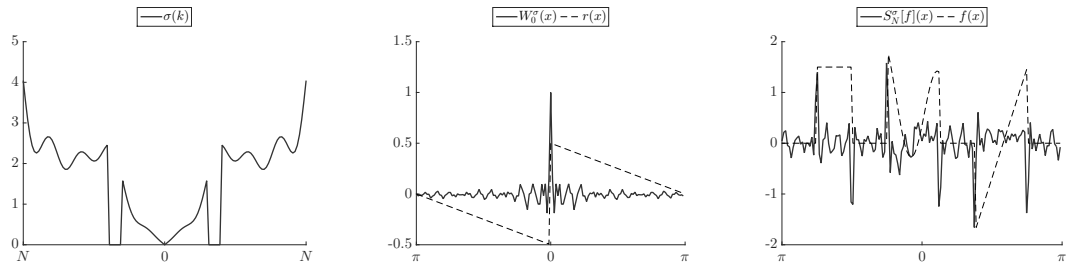


Since this design also allows for missing random frequencies of data, we will consider another problem formulation with a random subset of the frequency space $K \subset [-N, N]$ missing, where $|K| = \lfloor (0.1)(2N+1) \rfloor$ so that $\hat{f}_k = 0$ when $k \in K$, that is, about 10% of the spectral data are unknown.

**Problem Formulation 4**

$$\begin{aligned} \min_{\sigma} \quad & \left\| W_0^{\sigma}(x) \right\|_1 \\ \text{subject to} \quad & W_0^{\sigma}(x)\big|_{x=0} = 1, \\ & \left| W_0^{\sigma}(x) \right|_{|x|\geq 0.2} \leq 5 \times 10^{-2}, \\ & \sigma[K] = 0. \end{aligned} \tag{2.14}$$

This formulation leads to the concentration factor, jump response, and jump approximation as plotted in Figure 2.4. The missing frequencies are those values of $k$ where $\sigma(k) = 0$. The 1-norm is often useful in problem formulations where the objective function is to minimize something which is sparse, like the jump response. Thus the constraints in (2.14) are enforcing sparsity with quick decay.

Figure 2.4: Formulation 4 solution $\sigma$, $W_0^{\sigma}(x)$, and $S_N^{\sigma}[f](x)$, with $N = 64$.

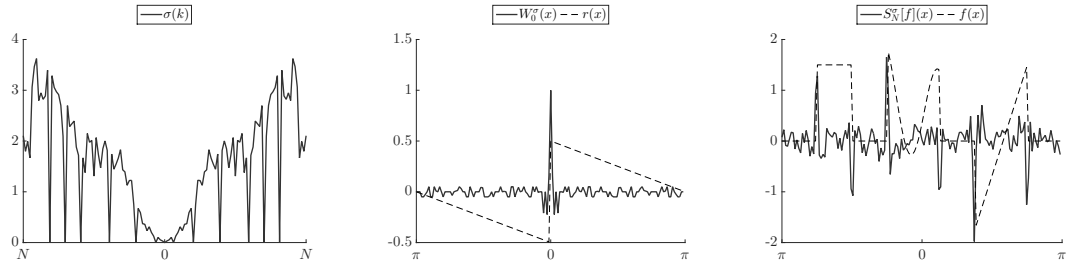

# Chapter 3

# Phase Data and Enhanced Edge Detection

The prior literature on concentration factors includes discussion on noisy and intermittent data. Additionally, non-uniform sampling schemes have been reviewed. However, in each of these approaches, the jump approximations are computed using both the phase and amplitude of the Fourier coefficients. Spectral magnitude and phase both carry information in a signal, but many important features are often found within the phase data itself. In particular, edges are found in the phase, and moreover, the phase relationships of spectral data determines the type of edges at a location in the signal [5]. Phase is thus not only useful for locating features in a signal, but also classifying them.

A common example of the difference in utility of phase and magnitude information is in x-ray crystallography, where measurements are only able to capture magnitude data. The structures cannot be built on this information alone, and hence there is extensive research in phase retrieval, where multiple measurements through masks are required to deduce some idea of the structure of the crystals.

Figure 3.1 demonstrates the importance of phase for edges in images. The spectral magnitude from Figures 3.1a and 3.1b are swapped, and then an inverse transform with the swapped magnitude gives Figures 3.1c and 3.1d. Notwithstanding the magnitude swap, the overall identifying structures in each image remains visible with the phase information.

Feature detection is still possible even when the magnitude information is distorted, modified, or even completely lost. Building on prior work, the concentration factor design method [7] allows the creation of concentration factors specifically targeted to approximate the jump function when given phase only information.

Figure 3.1: Scottish folk singer/songwriter Rachel Sermanni. First row: grayscale input images. Second row: reconstructions with swapped magnitude.

(a) Preprocessed grayscale image.

(b) Preprocessed grayscale image.

(c) Reconstruction using the phase from 3.1a and magnitude from 3.1b.

(d) Reconstruction using the phase from 3.1b and magnitude from 3.1a.

## 3.1 Edge Detection from Phase Data

Suppose $f$ is a $2\pi$-periodic function on $[-\pi,\pi)$ with a single jump discontinuity at $x = \xi \in (-\pi,\pi)$. From (2.5) and noting that

$$\frac{1}{i} = -i = e^{-i\frac{\pi}{2}},$$

we see

$$\hat{f}_k = \frac{[f](\xi)}{2\pi k} e^{-i(k\xi+\pi/2)} + O\left(\frac{1}{k^2}\right). \tag{3.1}$$

The magnitude and phase of these Fourier coefficients are then approximately given by

$$|\hat{f}_k| \approx \left|\frac{[f](\xi)}{2\pi k}\right| \text{ and } \varphi(\hat{f}_k) \approx -\left(k\xi + \frac{\pi}{2}\operatorname{sgn}\left(k\cdot[f](\xi)\right)\right). \tag{3.2}$$

respectively. As seen in (3.2), the jump location $\xi$ is encoded in the phase, while the jump height $[f](\xi)$ is encoded in the magnitude of the Fourier coefficients. Note that due to Euler's identity $e^{i\pi} = -1$, the sign of the jump and the sign of $k$ are also encoded in the phase.

The standard design approach reviewed in Section 2.1 looks for functions $\sigma$ which satisfy (2.3). Suppose $\sigma$ is such a concentration factor. We would like to explore the possibility of modifying this framework to develop concentration factors $\tilde{\sigma}$ which yield $[r](x)$ from (2.3) when the spectral magnitude is removed from the Fourier coefficients $\hat{r}_k$.

To that end, define

$$\tilde{r}_k := \begin{cases} \frac{\hat{r}_k}{|\hat{r}_k|} & k \neq 0, \\ 0 & k = 0. \end{cases} \tag{3.3}$$

If the jump response from full data is given by $W_0^{\sigma}(x)$, let the jump response built from phase data be defined as

$$W_0^{\tilde{\sigma}}(x) := \sum_{0<|k|\leq N} i\operatorname{sgn}(k)\tilde{\sigma}(k)\tilde{r}_k e^{ikx}. \tag{3.4}$$

If $\tilde{\sigma}(k) = \sigma(k)|\hat{r}_k|$, then

$$\sum_{0<|k|\leq N} i\operatorname{sgn}(k)\tilde{\sigma}(k)\tilde{r}_k e^{ikx} = \sum_{0<|k|\leq N} i\operatorname{sgn}(k)\sigma(k)|\hat{r}_k|\frac{\hat{r}_k}{|\hat{r}_k|}e^{ikx} = W_0^{\sigma}(x), \tag{3.5}$$

so $\tilde{\sigma}(k)$ is a concentration factor exactly giving $W_0^{\sigma}(x)$ from only the phase information $\tilde{r}_k$. As in (2.1), the Fourier coefficients of the ramp function are given by $\hat{r}(k) = 1/(2\pi i k)$ whenever $k \neq 0$ and $\hat{r}(0) = 0$. Removing the magnitude from the Fourier coefficients of the ramp function,

$$\tilde{r}_k = -i\operatorname{sgn}(k).$$

With $\tilde{r}_k$ and the concentration factor $\tilde{\sigma}$, (3.4) simplifies to

$$W_0^{\tilde{\sigma}}(x) = \sum_{0<|k|\leq N} \tilde{\sigma}(k)e^{ikx}.$$

Notice that when $\tilde{\sigma}(k) = 1$, this summation yields the Dirichlet kernel with a DC offset. If the concentration factor effectively normalizes the height, then this converges to a shifted Kronecker delta (1.6).

This concentration factor then can also yield an approximation $S_N^{\tilde{\sigma}}[f](x)$. It should be stated that the amplitude of the jumps in the partial sum approximation cannot be expected to be accurate, since we are not given amplitude data. In particular, the solutions assume that the magnitude of the Fourier coefficients are $1/(2\pi|k|)$. Since the Fourier coefficients of a piecewise-smooth function decay with $O(1/k^2)$, this assumption at least stays on the correct order of magnitude for the Fourier coefficients.

Thus, we can pose a problem formulation where only the spectral phase data $\hat{f}_k/|\hat{f}_k|$ is known, and recover the jumps $[f](x)$ of the underlying function.

**Problem Formulation 5**

$$\begin{aligned} \min_{\tilde{\sigma}} \quad & \left\| W_0^{\tilde{\sigma}}(x) - [r]_\epsilon(x) \right\|_2 + \lambda \left\| W_0^{\tilde{\sigma}}(x) \right\|_1 \\ \text{subject to} \quad & W_0^{\sigma}(x)\big|_{x=0} = 1. \end{aligned} \tag{3.6}$$

This gives a concentration factor $\tilde{\sigma}$ with the jump response and jump approximation shown in Figure 3.2 with $\lambda = 0.5$. Due to the missing information of the jump heights in the spectral data, only the jump locations are exact, while the jump heights are not properly scaled. Notice that that the jump response is identical to that from (2.12), the same problem formulation with full data.

Figure 3.2: Formulation 5 solution $\tilde{\sigma}$, $W_0^{\tilde{\sigma}}(x)$, and $S_N^{\tilde{\sigma}}[f](x)$ from Fourier phase data $\hat{f}_k/|\hat{f}_k|$, with $\lambda = 0.5$, $N = 64$.

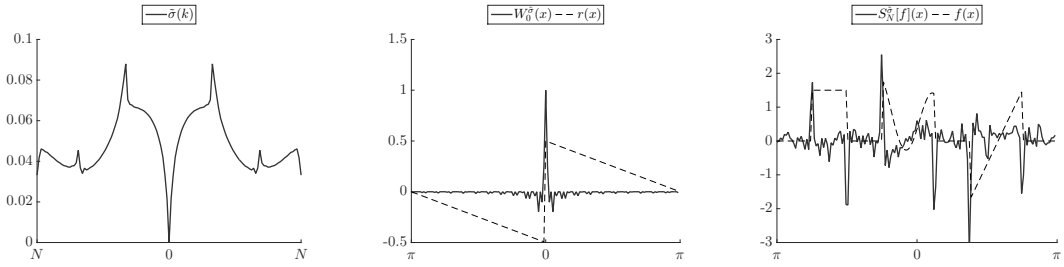


It can be seen in Figure 3.2 that there are some spurious jumps in the domain. Some false positives are expected when many harmonics either share the same phase (leading to step edges) or are out of phase by exactly $\pi/2$ radians (leading to delta edges) since phase congruency will be high at regular intervals in the domain [3] when the frequencies are weighted identically. This is exacerbated in the case of banded or intermittent data, where the set of missing frequencies will contain some which either add

to or suppress edges, and especially so with spectral phase data. This is exemplified in the following problem formulation, where only the spectral phase is given and the frequencies $K = \{k : 20 \leq |k| \leq 25\}$ are missing.

**Problem Formulation 6**

$$\begin{aligned} \min_{\tilde{\sigma}} \quad & \left\| W_0^{\tilde{\sigma}}(x) \right\|_1 \\ \text{subject to} \quad & W_0^{\tilde{\sigma}}(x)\big|_{x=0} = 1, \\ & \tilde{\sigma}[K] = 0. \end{aligned} \tag{3.7}$$

This problem formulation uses the 1-norm to get a sparse jump response with proper normalization, leading to a very distinct jump response which oscillates heavily around the jump location but decays quickly.

Figure 3.3: Formulation 6 solution $\tilde{\sigma}$, $W_0^{\tilde{\sigma}}(x)$, and $S_N^{\tilde{\sigma}}[f](x)$ from Fourier phase data $\hat{f}_k/|\hat{f}_k|$, with $\hat{f}_k = 0$ for $k \in K$, $N = 64$.

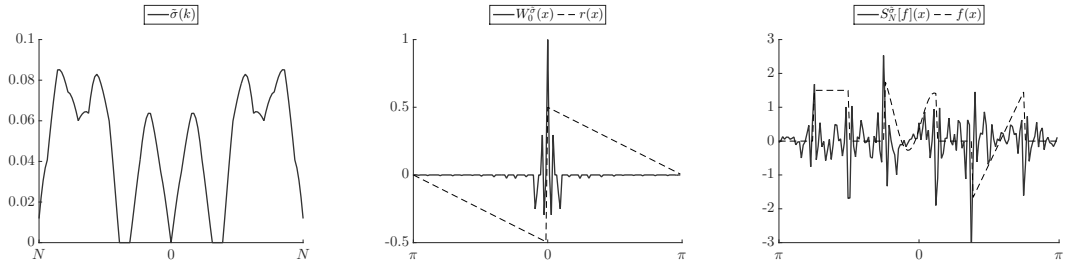


## 3.2 Multiple Concentration Factors

All of the problem formulations discussed give rise to some very different concentration factors, each with a signature jump response. One problem in jump reconstruction is that if we want a quicker convergence to the true jump function away from the discontinuities, then we receive stronger oscillations around the jumps. This is evidenced in the trigonometric and higher order exponential concentration factors from Figure 1.1. This is exacerbated if two discontinuities are relatively near each other, as the oscillations can interfere with the jump heights. Low order polynomial concentration factors have very low amounts of oscillations around the jumps, but slow convergence away from jumps. So, around the jump locations, we want behaviors like the low order edge

detectors, while farther from them, we want the quickly decaying behavior of higher order detectors. The method introduced in [2] uses a slope limiter to utilize the strengths of both low order and high order concentration factors.

The slope limiter used in [2] is the operator minmod$(\cdot)$, which removes spurious oscillations by setting the detector to zero when a set of concentration factors produce approximations with opposite signs, and takes the minimum of two detectors away from these oscillations. Precisely stated, the minmod operator applied to two functions $\phi_1, \phi_2$ over $x$ is defined by

$$\text{minmod}(\phi_1,\phi_2)(x) = \begin{cases} \text{sgn}\,\phi_1(x)\cdot \min\limits_{i=1,2}|\phi_i(x)| & \text{if sgn}\,\phi_1(x) = \text{sgn}\,\phi_2(x), \\ 0 & \text{otherwise.} \end{cases} \tag{3.8}$$

Note that the operator can be extended to handle more arguments $\phi_i$ for $i = 1,\ldots,n$ by composition, so that

$$\text{minmod}(\phi_1,\ldots,\phi_n)(x) = \text{minmod}\left(\text{minmod}(\phi_1,\ldots,\phi_{n-1})(x),\phi_n\right)(x) \tag{3.9}$$

The detector built from using the minmod operator on jump approximations from concentration factors $\sigma_1,\ldots,\sigma_n$ then is

$$MM_N^{\sigma_1,\ldots,\sigma_n}[f](x) := \text{minmod}(S_N^{\sigma_1}[f],\ldots,S_N^{\sigma_n}[f])(x). \tag{3.10}$$

To illustrate the effectiveness of the operator, consider its use on two jump approximations using the order 1 polynomial concentration factor $\sigma^P$ and the order 6 exponential concentration factor $\sigma^E$ from Table 1.1 (plotted in Figure 1.1). This will give the detector

$$MM_N^{\sigma^P,\sigma^E}[f](x) = \text{minmod}(S_N^{\sigma^P}[f], S_N^{\sigma^E}[f])(x), \tag{3.11}$$

which is shown in Figure 3.4 next to the two jump approximations. Notice that the minmod detector is zero in areas of oscillations between jumps, and is the minimum of the two jump approximations around the areas of jumps.

Spurious jumps are minimized after slope limiting, so thresholding techniques can be more effectually applied to the detector to create an *enhanced* edge detector to extract the exact jump locations. To do so, the scales of the small errors from the $O(1)$ jumps should be separated, and then thresholding can be applied to produce an explicit detector.

Let $f$ have discontinuities $\{\xi_j : j = 1,\ldots,n\}$ and suppose $S_N^\sigma[f](x)$ is a jump approximation of $f$ from an admissible concentration factor $\sigma$. Choose $q > 1$ and compute

$$E_{q,N}(x) := N^{q/2}(S_N^\sigma[f](x))^q \approx \begin{cases} N^{q/2}([f](\xi_j)^q & x = \xi_j, \\ O(N^{-q/2}) & x \neq \xi_j. \end{cases} \tag{3.12}$$

Figure 3.4: Minmod detector from approximations $S_N^{\sigma^P}[f](x)$ and $S_N^{\sigma^E}[f])(x)$, $N = 64$.

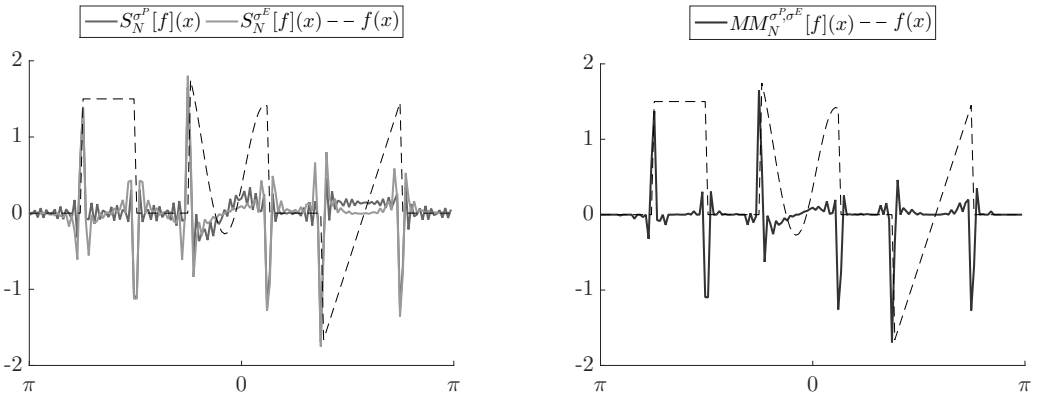


These values are then compared to some $O(1)$ threshold $\vartheta$ to produce the the enhanced thresholding detector

$$T_N^{\sigma}[f](x) := \begin{cases} S_N^{\sigma}[f](x) & |E_{q,N}(x)| > \vartheta, \\ 0 & |E_{q,N}(x)| \leq \vartheta. \end{cases} \tag{3.13}$$

The enhanced detector can be built from any jump approximation, but as stated previously, the removal of spurious jumps and oscillations from the minmod detector allows a clear separation of scales for better responses to thesholding. These post-processing techniques deliver an out of the box edge detector that performs exactly as we would hope to expect from clean data. Taking the minmod detector from (3.11) and applying the thresholding technique with $q = 2$ and $\vartheta = 30$, we generate the enhanced detector plotted in Figure 3.5 alongside the minmod detector.

It is not immediately obvious how to choose concentration factors so that the jump approximations will give the best results when combined via the midmod operator. We do know that in general, a lower order and higher order factor will yield different types of behaviors around and away from jumps, but it is not clear how to maximize this difference or how to choose more than two factors. Moreover, the limiter does not take into account any relationships the concentration factors may have. In [6], a hypothesis testing method was developed which exploited the relationship between edges in a jump approximation and the jump response from a concentration factor. By comparing the jump response in a neighborhood around the jump location to any stencil in the reconstruction domain, false positives can be rejected easily to build a strong detector. Furthermore, this method of hypothesis testing allows for testing a series of approximations from different concentration factors.

Figure 3.5: Enhanced detector $T_N^{\sigma^E,\sigma^P}[f](x)$ with $q = 2$, $\vartheta = 30$, $N = 64$.

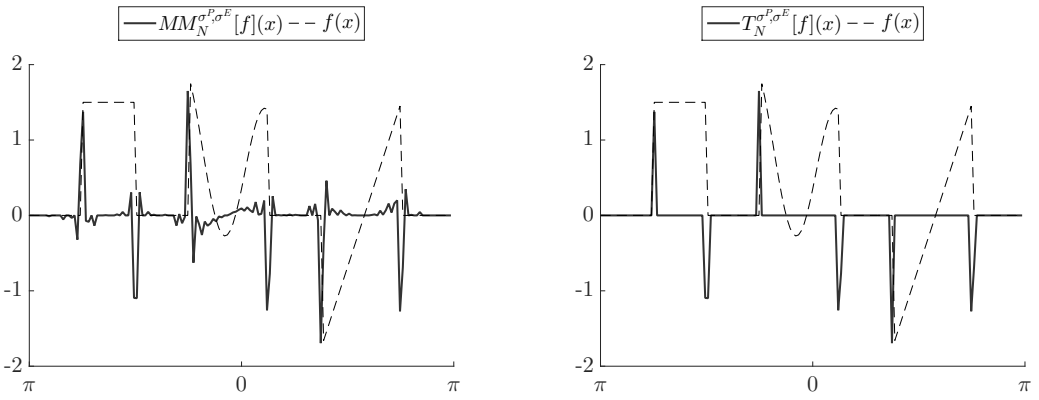


The use of different concentration factors results in a covariance structure of the jump approximations given by

$$C_{i,j}^{p,q} := \operatorname{cov}\left(S_N^{\sigma_p}(x_i), S_N^{\sigma_q}(x_j)\right) = \sum_{0<|k|\le N} \sigma_p(k)\sigma_q(k)e^{ik(x_i-x_j)}. \tag{3.14}$$

It is evident that if the inner product of two concentration factors is small, then so is the corresponding covariance between the jump detectors. That is, two concentration factors result in as different as possible jump approximations when the concentration factors are orthogonal. Those concentration factors then should be able to maximize the utility of post-processing schemes such as the minmod operator or statistical hypothesis testing. From the design perspective, if $\sigma_1$ is a concentration factor, a second concentration factor $\sigma_2$ can be built so that it is orthogonal to the first with the addition of a simple constraint. Consider the following formulation then, starting with the low order polynomial concentration factor $\sigma_1 = \sigma_{p=1}^P$.

**Problem Formulation 7**

$$\begin{aligned} \min_{\sigma_2} \quad & \left\| W_0^{\sigma_2}(x) \right\|_2 \\ \text{subject to} \quad & W_0^{\sigma_2}(x)\big|_{x=0} = 1, \\ & \langle \sigma_1, \sigma_2 \rangle = 0. \end{aligned} \tag{3.15}$$

This formulation leads to the concentration factors, jump responses, and jump approximations as plotted in Figure 3.6.

Earlier in (3.11) and plotted in Figure 3.4, the minmod operator was applied to the low order polynomial and high order exponential concentration factors. The minmod

Figure 3.6: Formulation 7 solution $\sigma_2$ and concentration factor $\sigma_1 = \sigma_{p=1}^P$, jump responses $W_0^{\sigma_1}(x)$, $W_0^{\sigma_2}(x)$, and jump approximations $S_N^{\sigma_1}[f](x)$ and $S_N^{\sigma_2}[f](x)$, $N = 64$.

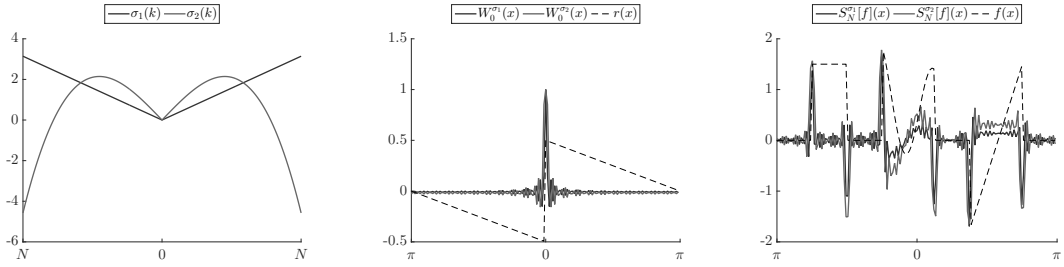


operator applied instead to the low order polynomial factor and the solution to formulation 7 gives a slight improvement around the jump locations to the former. Of course, these two detectors can also be passed through the minmod operator to yield $MM_N^{\{\sigma\}}[f](x)$ so that the reduced oscillations around the jump from (3.15) are taken in, while the smaller regions away from the jumps primarily are taken from (3.11). These three minmod detectors, from $\sigma_P, \sigma^E$ and $\sigma_1, \sigma_2$ and from the combination are plotted in Figure 3.7. The compositional minmod operator is already quite close to the exact jump detector, so thresholding on this even with a low threshold will result in an excellent detector like the one plotted in Figure 3.5.

Figure 3.7: Minmod operator on a number of jump approximations $\{\sigma\} = \{\sigma^P, \sigma^E, \sigma_2\}$, $N = 64$.

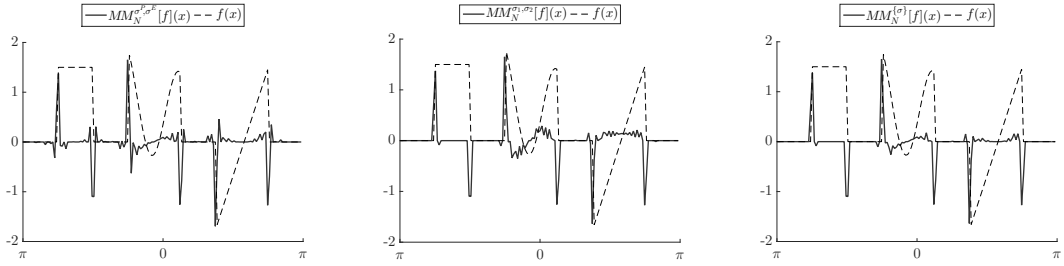


In almost any application, data are corrupted by at least some amount of noise. So we are not trying to recover the jump function from the exact Fourier coefficients, but instead noise affected data. Since spectral data are complex, the noise $\nu_k$ is simulated with complex additive white Gaussian noise with mean zero and variance $\rho^2$,

$$\hat{f}_k + \nu_k, \qquad \nu_k \sim \mathscr{CN}(0, \rho^2). \tag{3.16}$$

Since the concentration factor method is linear and the noise has mean zero, the concentration sum (1.8) with noisy data has the expected value

$$\mathrm{E}\left[S_N^\sigma[f+\nu](x)\right] = \mathrm{E}\left[\sum_{0<|k|\le N} i\,\mathrm{sgn}(k)\sigma(k)(\hat{f}_k+\nu_k)e^{ikx}\right] = S_N^\sigma[f](x). \tag{3.17}$$

Thus, the concentration factor method is robust to noise; on average the noise does not bias the reconstruction.

To show the extent of the discussed methods and their application to a scenario with the many problems of real data collection, we will consider spectral phase data that is corrupted by noise and interrupted in a band of frequencies. Multiple orthogonal concentration factors will be built to realize the missing frequencies, and then the approximations will be combined through the minmod operator, and finally thresholded. Thus in the following problem formulation, the obtained data has the form

$$\tilde{g}_k = \frac{\hat{f}_k+\nu_k}{|\hat{f}_k+\nu_k|} \tag{3.18}$$

with a signal-to-noise ratio of 12 dB. The data are additionally assumed to be unusable on $K = \{k : 15 \le k \le 20\}$ so that $\tilde{g}_k = 0$ when $k \in K$.

**Problem Formulation 8**

$$\begin{aligned}
\min_{\tilde{\sigma}_1} \quad & \left\| W_0^{\tilde{\sigma}_1}(x) \right\|_2 \\
\text{subject to} \quad & W_0^{\tilde{\sigma}_1}(x)\Big|_{x=0} = 1, \\
& \left| W_0^{\tilde{\sigma}_1}(x) \right|_{|x|\ge 0.2} \le 10^{-2}, \\
& \tilde{\sigma}_1[K] = 0, \\
\min_{\tilde{\sigma}_2} \quad & \left\| W_0^{\tilde{\sigma}_2}(x) \right\|_2 \\
\text{subject to} \quad & W_0^{\tilde{\sigma}_2}(x)\Big|_{x=0} = 1, \\
& \tilde{\sigma}_2[K] = 0, \\
& \langle \tilde{\sigma}_1, \tilde{\sigma}_2 \rangle = 0.
\end{aligned} \tag{3.19}$$

This problem formulation iterately solves for $\tilde{\sigma}_1$ and then iterately solves for an orthogonal $\tilde{\sigma}_2$. The solutions and their respective jump responses and jump approximations are shown in Figure 3.8.

Figure 3.8: Formulation 8 solutions $\tilde{\sigma}_1$ and $\tilde{\sigma}_2$ with jump responses and jump approximations from noisy Fourier phase data $\tilde{g}_k$ (3.18), with $\tilde{g}_k = 0$ for $k \in K$, $N = 64$.

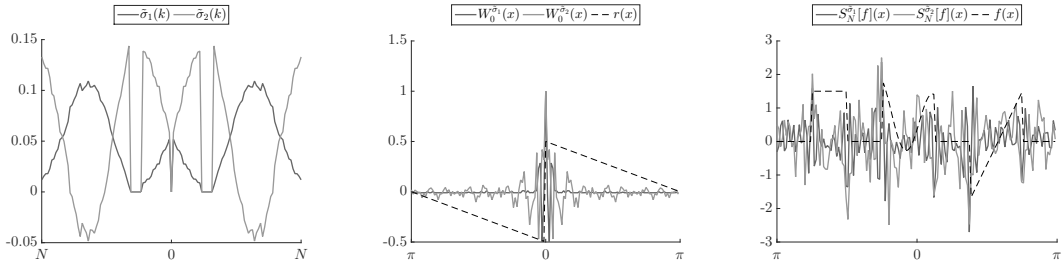


The two jump approximations are then passed into the minmod operator to remove spurious oscillations, and then finally thresholded to build the detector seen in Figure 3.9. Despite the relatively wild behavior of the jump approximations from such data, the minmod detector removes a substantial amount of the oscillations, and thresholding is still able to separate the scales of the jumps from the noise. The final detector, though not with accurate jump heights due to both the noise and the removal of the magnitude, is still able to make out a solid approximation to the jump function $[f]$.

Figure 3.9: Minmod detector $MM_N^{\tilde{\sigma}_1,\tilde{\sigma}_2}[f](x)$ and enhanced detector $T_N^{\tilde{\sigma}_1,\tilde{\sigma}_2}[f](x)$ with $q = 2$ and $\vartheta = 30$ from Formulation 8 solutions, $N = 64$. Compare this to the enhanced detector $T_N^{\tilde{\sigma}^P,\tilde{\sigma}^E}[f](x)$ from the analytic concentration factors $\tilde{\sigma}^P$ and $\tilde{\sigma}^E$ which assume data are given throughout $K$.

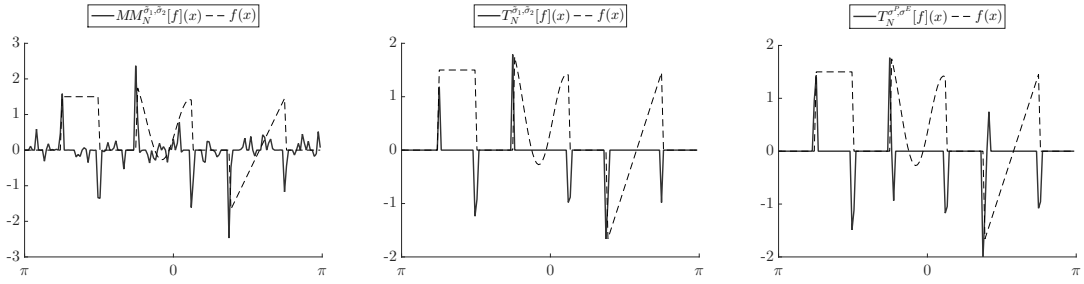


Finally, we will end this thesis with a problem formulation similar to the previous one, with phase-only data and missing frequencies, except in two dimensions on images. Images have many more edges than the functions that have been considered in this thesis. There are usually areas with many edges close together, and many of them have small amplitudes. This makes thresholding difficult, and wherever the edges are not sufficiently resolved, the oscillations in the detector near jumps make certain edges

difficult to clearly identify with the right height.

Often in two dimensions, spectral data are not sampled uniformly, but the following examples were kept to the simple case of uniform Fourier data sampled in two dimensions. Since the images called for a larger domain, the number of Fourier coefficients was also increased to 600 so that the frequency domain was on the interval $[-300, 299]$. Missing frequencies were assumed at $K = \{k : 120 \leq |k| \leq 150\}$. Aside from these two changes, the program was identical to Problem Formulation 8 (3.19). Due to these problems, a perfect edge map should not be expected from this data. The grayscale input and the enhanced edge detector output after thresholding are given in Figure 3.10. The enhanced edge detectors from full, uninterrupted data are also shown for comparison.

## 3.3 Concluding Remarks

This research originally set out to explore the possibilities of detecting edges from spectral phase data. The concentration factor method gives us some intuition and insight into the relationships between features in a signal and its spectral phase. With the understanding of the concentration factor design model, it was seen that a formulation could be posed within the framework to realize an edge detector from phase only data.

With a detector constructed, post-processing schemes relying on the difference of multiple edge approximations yielded an enhanced edge detector, which is shown to be rather robust under noisy, intermittent phase data. All of the work was then extended to two dimensions, where the processes were shown to perform well on image input.

Further avenues of work lie ahead for edge detection, especially in the statistical realm. Recently, [4] showed that the statistical hypothesis tests developed in [6] could be combined for many jump approximations for a post-processing scheme which relies less on thresholding techniques, and thus less on human intervention. Over the next summer, my research will focus on statistical techniques in signal processing, and I hope to revisit this work and extend the results from [4] using orthogonal factors as discussed in Chapter 3 of this thesis.

Figure 3.10: Scottish folk singer/songwriter Rachel Sermanni. First row: input grayscale images. Second row: enhanced detector after applying a minmod operator to two approximations and thresholding. Third row: enhanced detector from spectral phase data with missing frequencies $K$. Thresholding parameters $q = 5$ and $\vartheta = 1$, $N = 300$.

(a) Preprocessed grayscale image.

(b) Preprocessed grayscale image.

(c) Edge detection on 3.10a, full data.

(d) Edge detection on 3.10b, full data.

(e) Edge detection on 3.10a from band interrupted phase data.

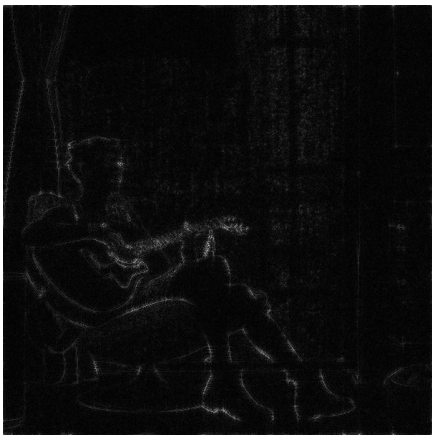

(f) Edge detection on 3.10b from band interrupted phase data.

# Bibliography


[1] A. Gelb and E. Tadmor. Detection of Edges in Spectral Data. *Applied and Computational Harmonic Analysis*, 7(1):101–135, 1999.

[2] A. Gelb and E. Tadmor. Adaptive Edge Detectors for Piecewise Smooth Data Based on the minmod Limiter. *Journal of Scientific Computing*, 28(9):279–306, 2006.

[3] P. Kovesi. Image Features from Phase Congruency. *Videre: Journal of Computer Vision Research*, 1(3):1–26, 1999.

[4] S. Lubold. A Statistical Framework for Detecting Edges from Noisy Fourier Data Using Multiple Concentration Factors. *Arizona State University*, Honors Thesis, 2015.

[5] Alan V. Oppenheim and Jae S. Lim. The Importance of Phase in Signals. *Proceedings of the IEEE*, 69(5):529–541, 1981.

[6] A. Petersen, A. Gelb, and R. Eubank. Hypothesis Testing for Fourier Based Edge Detection Methods. *Journal of Scientific Computing*, 51:608–630, 2012.

[7] A. Viswanathan, A. Gelb, and D. Cochran. Iterative design of concentration factors for jump detection. *Journal of Scientific Computing*, 51(3):631–649, 2012.